PHYSICAL REVIEW C VOLUME 2, NUMBER 4 OCTOBER 1970

Double-Energy Single-Time-of-Flight Measurements of Fission Fragments in Thermal-Neutron-Induced Fission of U^{235}†

Mary Derengowski and E. Melkonian
Pegram Nuclear Physicas Laboratory, Columbia University, New York, New York 10027
(Received 5 January 1970)

An experiment has been performed on the thermal-neutron-induced fission of U^{235}, in which the energies of complementary fission fragments and the time of flight of one fragment were measured. Fragment masses after neutron emission were obtained directly from this information. Pre-neutron masses and kinetic energies were deduced by means of a reflection method which simulates a double-time-of-flight experiment. Subtraction of post-neutron from primary fragment masses then gave the number of neutrons emitted by single fragments in each event. Among the results presented are the distributions of the numbers of neutrons emitted by single fragments of fixed mass. This information is very difficult to obtain from other types of experiments, and there has been no previous publication of such results for any fissioning nucleus. The results also include the average number of neutrons emitted as a function of mass and total kinetic energy, as well as mass distributions in fixed kinetic energy intervals, and total kinetic energy distributions at fixed fragment masses.

INTRODUCTION

Until recently, all determination of the masses of primary fission fragments, that is, of the fragments before the emission of prompt neutrons, have been made by measuring either the energies or the velocities of complementary fission fragments and applying the momentum conservation law to the fissioning system. If there were no prompt-neutron emission, this procedure would be exact. The emission of prompt neutrons necessitates further assumptions before deducing primary masses from the measurements. In the double-velocity case, it is sufficient to assume that prompt-neutron emission is isotropic in the c.m. system of the fragments. The double-energy measurement requires, in addition, the application of corrections[1] depending on details of the neutron emission as a function of fragment mass.

The fact that the primary fragments are formed with sufficient excitation energy to emit one or more prompt neutrons implies that one needs to know more than the primary mass division in order to understand the fission process. To obtain more information, it is necessary to determine at least one parameter in addition to those measured in the primary mass determinations. In the present experiment, we have chosen to measure the energies of both complementary fission fragments together with the time of flight of one fragment. The availability of this third item of information makes it possible, with few assumptions, to determine the correlated fragment masses and energies both before and after neutron emission, and to deduce from these results details of neutron emission from individual fragment masses.

Primary masses in this experiment are obtained from the measured time of flight by a reflection method which simulates a double-time-of-flight experiment. The pre-neutron kinetic energies can then be deduced from the velocities and the calculated primary masses. The post-neutron masses are obtained directly from the measured energies and velocities of single fragments, while the number of emitted neutrons in each event is simply the difference between the primary and post-neutron masses. The precision of the primary mass determination is limited by the effect of prompt-neutron emission on the velocities which are measured. This introduces an intrinsic resolution smearing, in addition to that produced by experimental uncertainties. The post-neutron mass determination, however, is independent of neutron-emission effects and could, in principle, be made with arbitrary accuracy. The ultimate limitation on the post-neutron mass determination in the present experiment is the intrinsic energy resolution of the solid-state detectors for fission fragments and the experimental errors of measuring fragment velocities.

In recent years, Schmitt and his collaborators have been carrying on a series of double-energy single-time-of-flight experiments on various fissioning systems, namely, spontaneous fission of Cf^{252} [2] and the 13-MeV proton-induced fission of Ra^{226} [3] and U^{233}.[4] These experiments are similar in principle to the present experiment, but differ in some details of procedure and analysis.

There have been several experiments of various types on thermal-neutron-induced fission of U^{235}, the results of which can be compared with some of the results of the present experiment. The first is a double-energy double-time-of-flight measure-

ment performed by a group at Aldermaston.[5,6] In the reported results, they present primary and post-neutron heavy-fragment mass distributions as a function of the kinetic energy of the heavy fragment. They observe some structure in the primary mass distributions, but no additional structure produced by neutron emission.

Two other experiments which are related to the present results employ direct detection of neutrons in coincidence with fission fragments. The first is a triple-time-of-flight measurement performed by Milton and Fraser,[7] in which the time of flight of both the fragments and the coincident neutrons are measured. In addition, the neutron counters define the direction of emission of the neutron relative to the path of the fragment. Only preliminary results have been published, but the experiment is, in principle, capable of providing a great deal of information on the fission process. In the second neutron counting experiment, Maslin, Rodgers, and Core[8] (hereafter referred to as MRC) measured the energies of the fragments by means of solid-state detectors, while detecting the neutrons in a spherical liquid scintillator. This enabled them to obtain the number of emitted neutrons as a function of both fragment mass and total kinetic energy.

The present experiment furnishes an independent check of the direct neutron counting results by an entirely different method. We believe that the primary mass resolution in this experiment ($\sigma \sim 0.8$ amu) is superior to that which can be obtained by means of double-energy measurements such as MRC.

An important advantage of our indirect neutron-emission determination over the direct neutron counting experiments lies in the limited efficiency for neutron detection in the latter type of experiment. In the MRC experiment, for example, the efficiency for detecting neutrons from single fragments was about 50%. What this means, in practice, is that the result in any given event is ambiguous. One cannot distinguish an event in which no neutron was emitted from one in which the emitted neutron was not detected. This does not affect the average neutron-emission results if correct normalization procedures are carried out. However, it makes it very difficult, if not impossible, to perform the kind of event by event analysis which, in our case, results in distributions of the number of emitted neutrons by single fragments of fixed mass. These distributions are indirectly related to fragment-excitation-energy distributions. Although we cannot establish the excitation energies

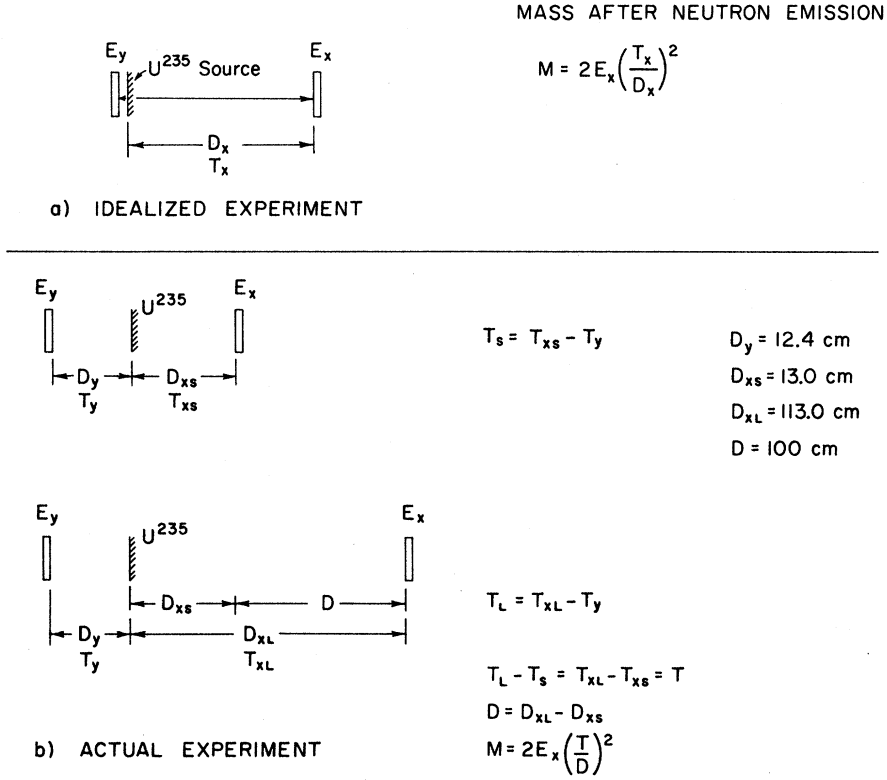

FIG. 1. Diagram of the time measurement in an idealized experiment (a) and in the actual experiment (b).

uniquely, it is still possible from our results to gain a qualitative understanding of the way in which the excitation energy is divided between the fragments.

EXPERIMENTAL PROCEDURE

A. General Method

A thin U^{235} source (30 $\mu g/cm^2$ on 100-$\mu g/cm^2$ nickel backing) was placed in an evacuated tube between two solid-state detectors. Fission was induced by a beam of thermal neutrons in the patient facility of the Brookhaven medical research reactor. Three quantities were recorded for each fission event: the energies of both complementary fragments and the time between the arrivals of the two fragments at the detectors, which was measured by a time-to-pulse-height converter. The two energy pulses and the output pulse from the time-to-pulse-height converter were analyzed by three analog-to-digital converters (ADC's) of a Radiation Instrument Development Laboratory (RIDL) three-parameter data acquisition system, and the resulting channel numbers were transferred, event by event, to magnetic tape.

In order to obtain from the time data the information which we needed for the mass calculations, namely, the time of flight of one fragment, we used a method which is illustrated schematically in Fig. 1. Figure 1(a) shows the arrangement of an idealized experiment, in which the distance is zero from the source to the detector which starts the time-to-pulse-height converter. Consequently, the measured time in this case is the time of flight of one fragment from the source to the stop detector. In the actual experiment, Fig. 1(b), the start detector was placed 5 in. from the source in order to keep it out of the main neutron flux and to reduce the singles rate from this detector. The time measured was then $T_x - T_y$, which involves both fragments instead of only one. We were able to eliminate the quantity T_y by performing two experiments in which only the distance to the stop detector was varied. The measured times in the two experiments were subtracted from each other. Then the result depended only on the velocity of the fragment detected by the stop detector and the difference between the flight-path lengths in the two runs. The short- and long-flight-path lengths were 12.7 and 112.7 cm, giving a difference in flight path 100.0 cm long. The present results were obtained from 60 000 events each, in the short- and long-flight-path runs.

One unique feature of the experiment was the elimination of timing walk due to fragment pulse-height variation. This was done by taking the time differences between events for which the pulse heights were very similar. Since the pulse-height contribution to the measured time was the same in both runs, it cancelled out in the subtraction.

B. Electronics

The electronic equipment consisted of two similar systems from which the energy measurements were obtained, and a timing system which measured the time interval between the detection of the two complementary fragments. Figure 2 is a block diagram of the system.

The separation between the energy and timing measurements was made immediately at the detector output by means of the transformer at the input of the ORTEC time-pickoff unit. The main portion of the pulse passed directly through the primary of the transformer to the input of a charge-sensitive preamplifier. After the preamplifier, the pulse was shaped and further amplified before entering the ADC.

Timing of the fission fragments was done on the small, fast-rising pulses produced and amplified within the time-pickoff units. After passing through buffer circuits, these pulses went to the time-to-pulse-height converter, which measured the time interval between them. The converter output pulse was amplified by a double-differentiating RC amplifier before entering the three-parameter system. The pulses from the nearby detector were delayed about 200 nsec by a length of cable between the time-pickoff unit and the control unit. This enabled us to use the lower-rate signal to start the converter, thus avoiding the pileup problems that would have resulted from an excessive start-input rate.

The three-parameter system accepted an event for analysis whenever its internal coincidence circuit detected pulses at the inputs of all three ADC's within an interval of 0.5 μsec. The channel numbers were then transferred from the scalers through an interface unit to a Digi-Data incremental magnetic tape unit. The timing information analyzed by one ADC was monitored during the experiment by means of an RIDL 400-channel analyzer and an interface circuit which has been described elsewhere.[9]

C. Time-Calibration Procedure

The primary standard for calibrating the time-to-pulse-height converter was the 50-MHz signal produced by a Tektronix time-mark generator. The technique has been described in a commercial publication by E. G. & G.[10] The start input of the converter is triggered by the coincidence between the 50-MHz train and the random pulses from a

scintillation counter which is exposed to a radioactive source. A 10-kHz signal which is synchronized with the 50-MHz train is used to trigger the stop input. When the converter output is fed into a multichannel analyzer, the spectrum consists of a series of peaks. The separation between successive peaks corresponds to 20 nsec in time.

After the time-to-pulse-height converter was calibrated in this fashion, we used it to measure the electrical length of a set of delay cables, which then became our secondary timing standards. The set of delay cables was used between experimental runs and after the experiment was completed to calibrate the time-to-pulse-height converter and ADC throughout the range in which data were taken. This was done by supplying a pulser signal to the start and stop inputs of the converter, and delaying the stop relative to the start by inserting calibrated cables.

The two ADC's of the three-parameter system which were used for the pulse-height measurement were checked for linearity by means of a precision pulser. These results were fitted to a second-degree polynomial by a least-squares method. The time and the observed pulse heights were corrected for the small observed nonlinearity in the first stage of data analysis.

DATA ANALYSIS

The raw data for each event consisted of three channel numbers corresponding to a pulse height from each solid-state detector and the output of the time-to-pulse-height converter. The event-by-event analysis can be summarized as follows: From the raw data we obtained the energies of both

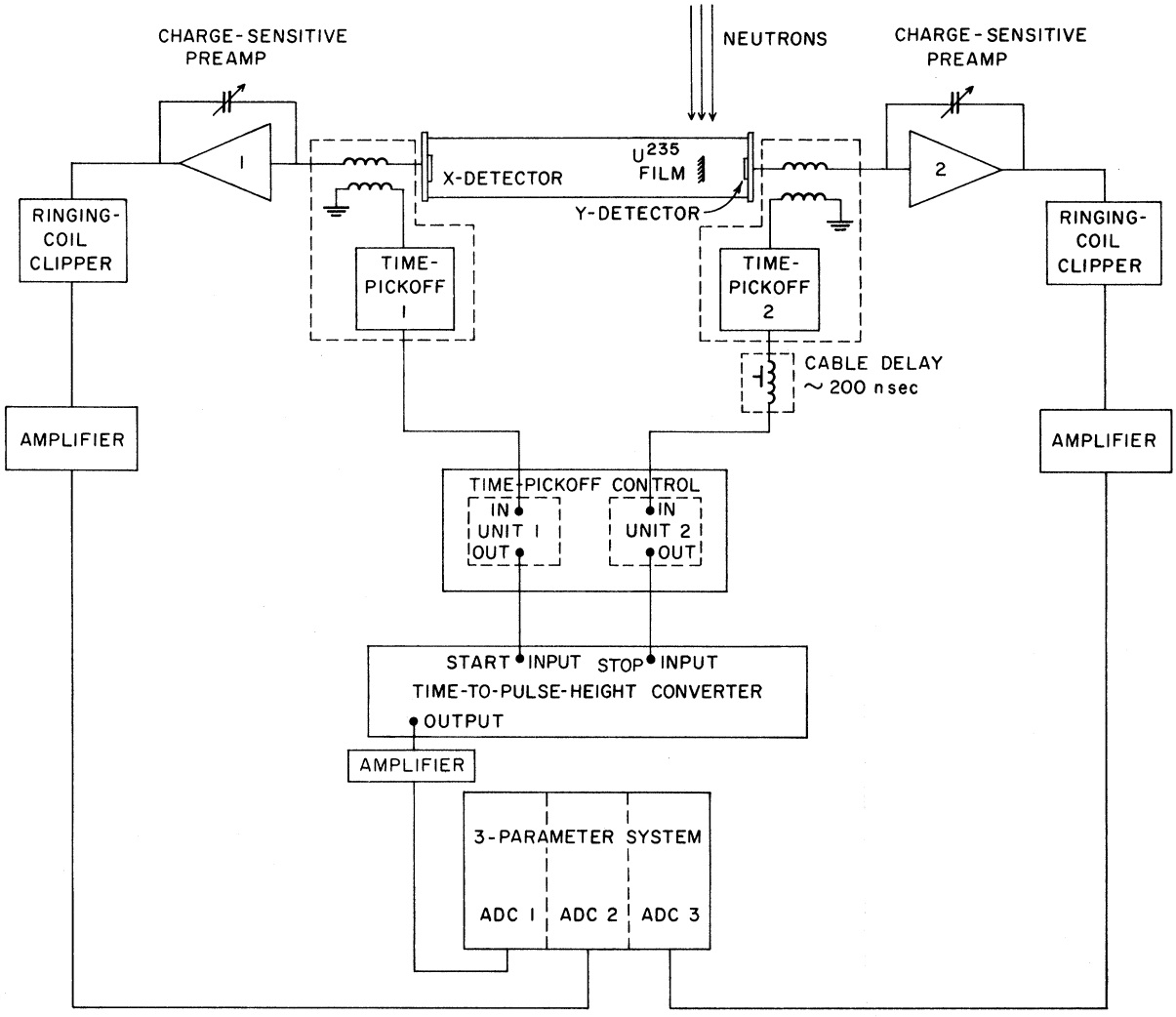

FIG. 2. Block diagram of the experimental electronic arrangement.

fission fragments and the time of flight of one. The post-neutron mass of one fragment was obtained from the energy and time of flight of that fragment. Pre-neutron masses were calculated from the time-of-flight information by a reflection method which is described below. Subtraction of the post-neutron from the pre-neutron mass then gave the number of neutrons emitted by one of the fragments. The computer used for analysis was the Columbia University IBM 7094.

A. Post-Neutron Masses

The energy of each fragment was obtained from the observed pulse height by means of the mass-dependent energy formula of Schmitt *et al.*[11]

$$E = (a + a'M)X + b + b'M \,, \tag{1}$$

where X is the observed pulse height. The constants a, a', b, and b' were obtained from the fission spectrum according to the procedure given in Ref. 11. The "a" coefficient, however, was reduced by 2.5%, and the other three coefficients were adjusted accordingly, in order to improve the agreement of the resulting post-neutron mass distribution with the radiochemical results summarized by Katcoff and quoted by Hyde.[12] The mass M which appears in Eq. (1) was obtained by iteration.

After the calculation of the fragment energies, the time differences between short- and long-flight-path runs were obtained as follows. The data from the short flight path run were sorted into a 1-by-1-MeV grid on the basis of the energies of the complementary fragments. The average-time channel for events in each box was calculated and stored in the computer memory. Then, as each event from the long flight path was analyzed, the program located the corresponding average time from the short-flight-path run as determined by the two energies. The time in the long-flight-path run was subtracted from the average time, giving the time of flight of the fragment over the difference flight path of 1 m.

Given the energy and the time difference, the post-neutron mass was obtained from the relationship

$$M = 2E(T/L)^2 \,, \tag{2}$$

where E is the measured post-neutron energy, T is the time difference, and L is the difference flight path length.

B. Primary Masses and Neutron Emission

The usual methods of obtaining the primary masses of fission fragments are based on the conservation of momentum and mass number between the fragments before they emit neutrons. These conditions give, for the pre-neutron mass of one fragment,

$$M = AV_2/(V_1 + V_2) \,, \tag{3}$$

where A is the mass of the fissioning nucleus and V_1 (V_2) is the velocity of fragment 1 (2) before the emission of neutrons.

If the neutrons are emitted isotropically in their own c.m. system by the fully accelerated fragments, which seems to be very nearly true, the velocity of the fragments should, on the average, be unchanged by neutron emission, and Eq. (3) should hold even for post-neutron velocities.

In the present experiment, the velocity of only one fragment is measured. However, because we also recorded the energies of both fragments, we were able to identify a class of events which were nearly complementary to any event we actually observed. The velocity of the complementary fragments was then identified as V_2.

The first step in the process is the sorting of all the events in the long-flight-path run into a two-dimensional energy grid, calculating the average time difference in each box and storing the results. Then the long-flight-path results are reanalyzed as follows. Each event is characterized by the measured energies EX and EY, and by T_1, the time difference. The energies determine in which box of the 1-by-1-MeV energy grid the event belongs. They also determine the box which contains the complementary events; i.e., the box with the values of EX and EY are interchanged. The average time calculated for this box is then taken as the time of flight of the complementary fragment. In this way, we simulated a double-time-of-flight experiment over two equal flight paths of 1 m. For this case, Eq. (3) becomes

$$M_1 = 236T_1/(T_1 + T_2) \,, \tag{4}$$

where M is the pre-neutron mass of fragment 1, T_1 is the measured time of flight of fragment 1, and T_2 is the average time of flight at the reflected point.

The energies of the fragments before neutron emission were calculated from the pre-neutron masses and the flight times:

$$\begin{aligned} E_1 &= \tfrac{1}{2}M(L/T_1)^2 \,, \\ E_2 &= \tfrac{1}{2}(236 - M)(L/T_2)^2 \,. \end{aligned} \tag{5}$$

The number of neutrons emitted by a fragment in

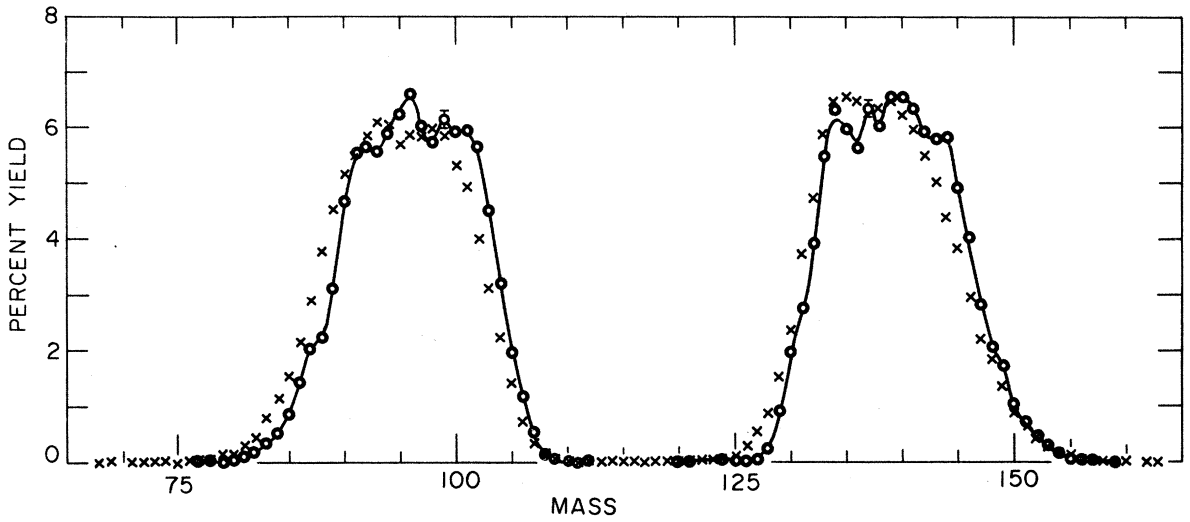

FIG. 3. Primary and post-neutron mass yields. Error bars indicate statistical error. Circles; pre-neutron mass. Crosses; post-neutron mass.

a given event was obtained by subtracting the post-neutron mass from the primary mass.

RESULTS AND DISCUSSION

After analysis each event is characterized by four main kinds of information: the pre-neutron masses of both fragments, the post-neutron mass of one fragment, the number of neutrons emitted by one fragment, and the energies of both fragments before neutron emission. There are many possible ways in which such results can be summarized. We have chosen primary fragment mass and total kinetic energy as the main parameters, and we examine the behavior of the results with one of these parameters fixed while the other is allowed to vary.

The primary and post-neutron mass distributions are shown in Fig. 3. Our method of calculating pre-neutron masses discriminates somewhat

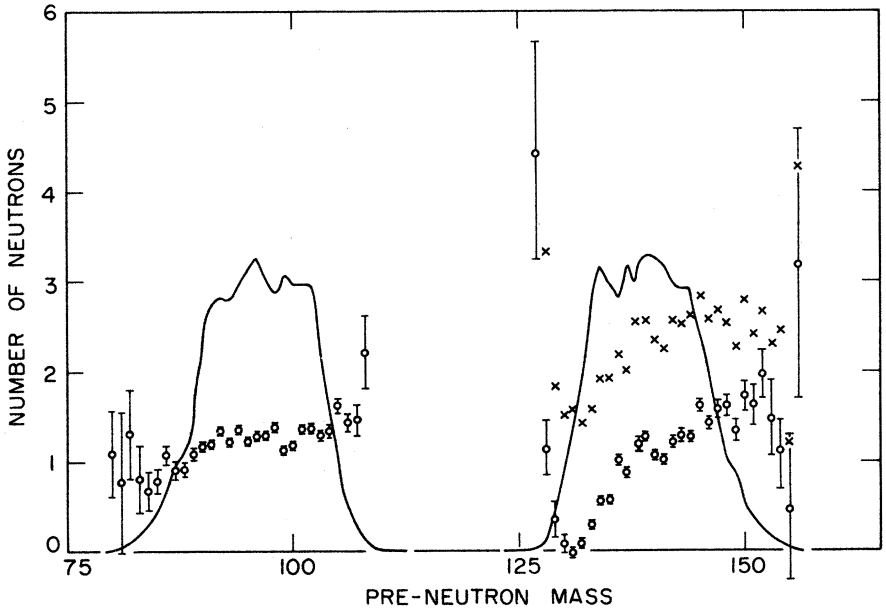

FIG. 4. Average neutron emission as a function of primary fragment mass. Error bars include only statistical error. The total neutron emission is the sum of the single-fragment values for complementary mass pairs. The pre-neutron mass distribution is shown for reference. Circles; single-fragment neutron emission. Crosses; total emission from fragment pair.

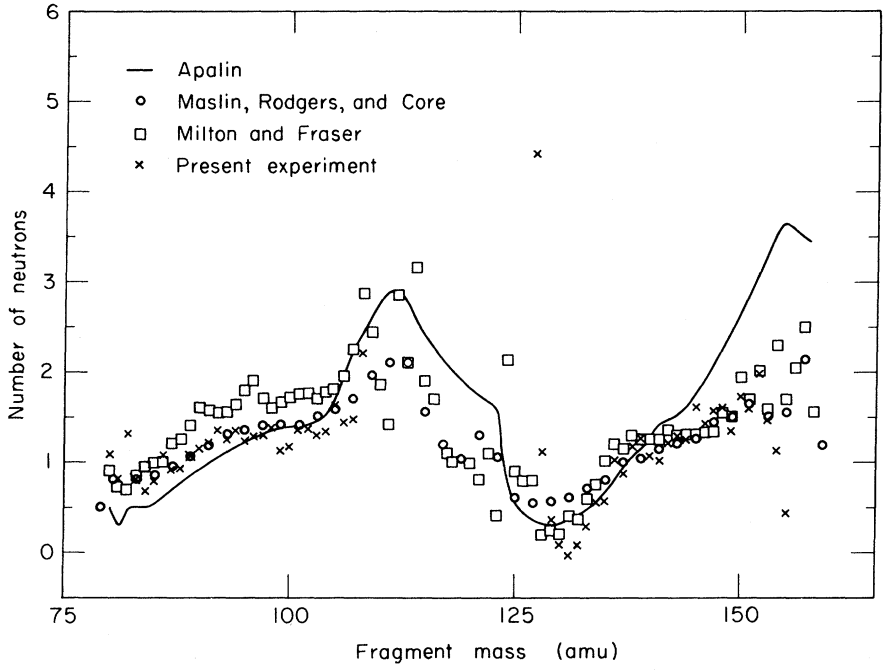

FIG. 5. Comparison of average neutron-emission results of the present experiment with those obtained in the direct neutron-counting experiments of MRC (see Ref. 8), Milton and Fraser (see Ref. 7), and Apalin *et al.* (see Ref. 14). *et al.* (see Ref. 14).

against events in the valley of the mass distribution, because an event is rejected unless there is at least one event in the reflected box. However, the minimum peak-to-valley ratio, even if we assume that all these rejected events were genuine, is about 1000 to 1, with uncertainty of 25%.

We estimate the resolution in the pre-neutron mass as a standard deviation of 0.8 to 0.9 amu, and in the post-neutron mass, between 0.6 and 2.2 amu, depending on the mass number. The post-neutron mass dispersion is about 0.8 amu at the center of the light-fragment peak, and about 1.6 amu at the center of the heavy-fragment peak. In calculating the resolution of the post-neutron mass determination, we have used a value of 1.5 MeV for the energy resolution full width at half maximum (FWHM) of the solid-state detectors, and a time resolution of 0.7 nsec FWHM. The latter fig-

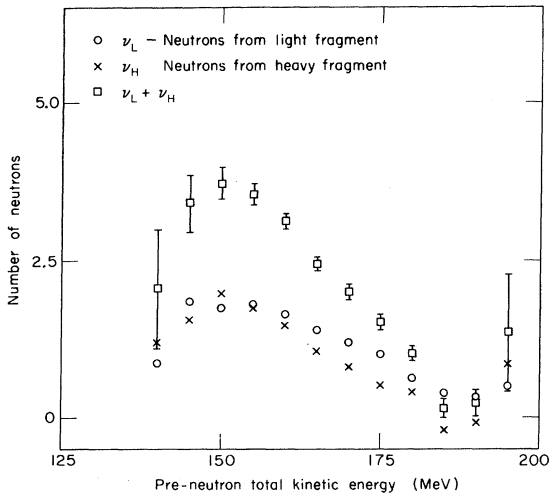

FIG. 6. Average neutron emission as a function of the total kinetic energy of the primary fragments.

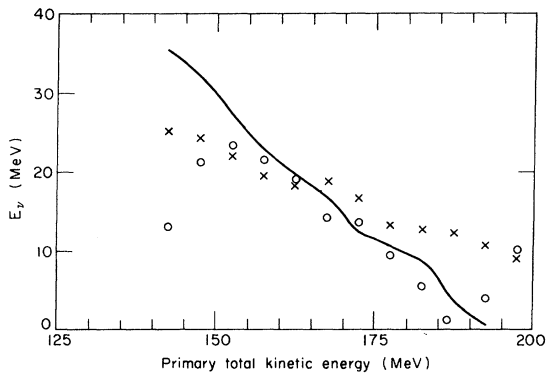

FIG. 7. Energy appearing in the form of prompt neutrons, as a function of primary total kinetic energy. Solid line; calculated from Ref. 14. Circles; present experiment. Crosses; results of MRC.

ure was obtained from the results of the short-flight-path run, in which the observed widths for events in a 1-by-1-MeV box of the two-dimensional energy grid gives an upper limit for the time resolution of the system. The post-neutron mass resolution is unaffected by neutron-emission effects, and the above-mentioned time resolution includes only experimental resolution smearing. On the other hand, in the pre-neutron mass resolution the neutron-emission effects predominate, contributing about 1.9 nsec FWHM at the light-fragment peak position, and 2.8 nsec at the heavy-fragment peak position.[13]

The average neutron emission as a function of fragment mass is shown in Fig. 4. The total neutron emission is simply the sum of the single-fragment results for complementary mass pairs. The solid curve is the pre-neutron mass distribution. In Fig. 5, the results of the present experiment are plotted along with the results of Maslin, Rodgers, and Core,[8] Milton and Fraser,[7] and Apalin *et al.*[14] On the whole, the present experiment agrees best with the data of MRC. The main discrepancy occurs near the doubly magic nucleus of mass 132, where we observe almost no neutron emission, a not unlikely result.

Figure 6 shows the average number of neutrons emitted as a function of fragment total kinetic energy. In the linear portion of the total-neutron-emission curve, between 150 and 185 MeV, the slope is one neutron per 11-MeV decrease in total kinetic energy. This is apparently in disagreement with the value obtained by MRC, which was one neutron per 18 MeV. There is, in our results, a drop in neutron emission at low total kinetic energies. MRC also see a falling off at the low-energy end, but it appears some 10 MeV lower than in our results.

We have done a calculation in which we compare the results shown in Fig. 6 and the corresponding results of MRC with those to be expected from consideration of the energy available for neutron emission. For this purpose, we have used Milton's tables[15] of total energy release and neutron binding energy, calculated from Cameron's mass formulas at each value of mass and charge division. Our procedure is as follows: At each value of total kinetic energy the average light- and heavy-

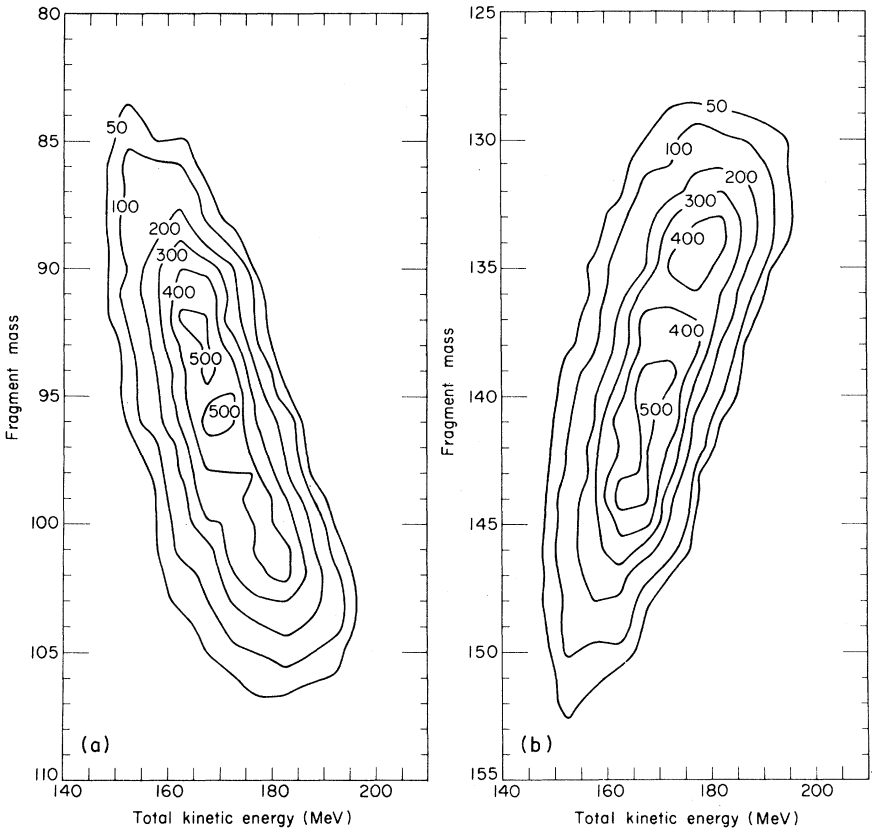

FIG. 8. Contour diagrams of the distribution of events as a function of primary fragment mass and primary total kinetic energy. The number attached to the contour corresponds to events (60 000 fissions)$^{-1}$ (mass unit)$^{-1}$ (5 MeV)$^{-1}$. (a) Light fragment. (b) Heavy fragment.

fragment mass obtained from the present results determines the mass division used in the calculation. From Milton's tables, we choose the charge division at that particular mass division which produces the maximum total energy release. The neutron binding energies of the fragments are also read off at this same charge division. The solid curve in Fig. 7 is the energy available for neutron emission. It is obtained by subtracting from the maximum energy release at each value of total kinetic energy the sum of the total kinetic energy and the energy carried off by γ rays. The value used for the γ energy was a constant 6 MeV.[16]

In order to make the comparison with our results, we assumed that the energy going into neutron emission at each total kinetic energy was

$$E_\nu = \nu_l (\text{B.E.}_l + 1.2) + \nu_h (\text{B.E.}_h + 1.2) , \qquad (6)$$

where ν_l (ν_h) = the average neutron emission from the light (heavy) fragment, B.E.$_l$ (B.E.$_h$) = the neutron binding energy of the light (heavy) fragment, at the division giving maximum energy release. The 1.2 MeV is the average neutron kinetic energy in the fragment c.m. system.[17] In this rather rough calculation, we have neglected the fact that this binding-energy value is correct only for the first neutron emitted. The results of this calculation appear as circles in Fig. 7.

We have attempted to make a similar calculation using the MRC results, with our own values for the mass division, and the same neutron binding energies as in the previous calculation. In the MRC paper, the results are given as the average number of neutrons per fragment, rather than heavy- and light-fragment emission separately. Accordingly, our calculated energies in this case were

$$E_\nu = \bar{\nu}(\text{B.E.}_l + \text{B.E.}_h + 1.2) , \qquad (7)$$

where $\bar{\nu}$ = the average number of neutrons per fragment at each total kinetic energy. The results of this calculation appear as crosses in Fig. 7.

Through most of the total kinetic energy range, the present results seem to follow the calculated curve in Fig. 7 more closely that the MRC results. We interpret this agreement as an indication that our value of 11 MeV per neutron is a reasonable result. The discrepancy below 150 MeV could re-

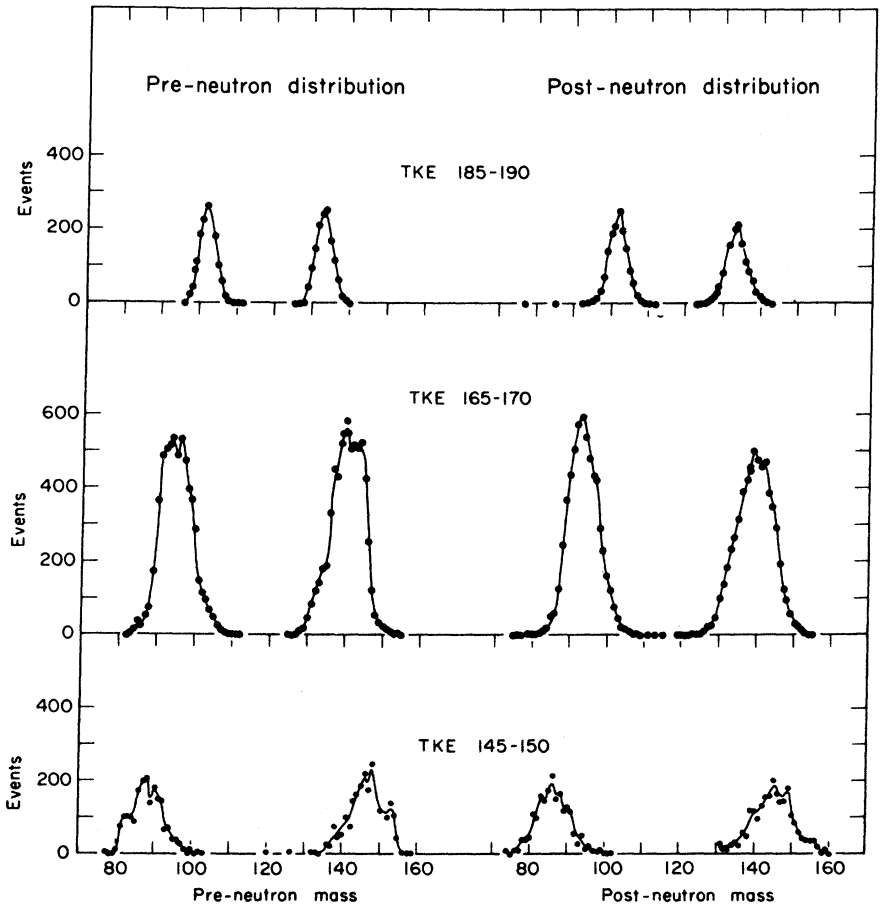

FIG. 9. Primary and post-neutron mass distributions at selected values of primary fragment total kinetic energy.

sult from a division of charge that does not result in maximum energy release. A shift of one or two charge units could easily account for the observed dip in neutron emission in Fig. 6.

Much of the information obtained in this experiment is a function of two parameters. This includes the mass distributions at fixed values of kinetic energy, the average neutron emission as a function of both mass and total kinetic energy, and the distributions of the number of neutrons emitted by single fragments of given mass.

Figure 8 is a contour diagram of primary mass yield versus total kinetic energy. Some representative mass distributions appear in Fig. 9. The upper, middle, and lower distributions are taken, respectively, from the high end, the peak, and the lower end of the total-kinetic energy distribution. The corresponding post-neutron mass distributions are also shown. Upon consideration of the whole series of pre-neutron mass distributions, we find evidence for a slight preference for fission into mass pairs with heavy fragments of 134, 140, 146, and 153 mass units. It does not appear from the post-neutron distributions that any additional structure is produced by neutron emission, although it is true that less than prominent structural features would be somewhat washed out by dispersion effects.

Our estimates of the magnitude of the mass dispersion indicate that the effect of resolution on the widths of the mass distributions such as those shown in Fig. 9 is, in most cases, rather small. The narrowest of the observed pre-neutron distributions has an observed width which corresponds, roughly, to a standard deviation of 2 amu about the peak. When one subtracts out the effect of a calculated mass dispersion of 0.9 amu, one is left with a standard deviation of about 1.8 amu for the

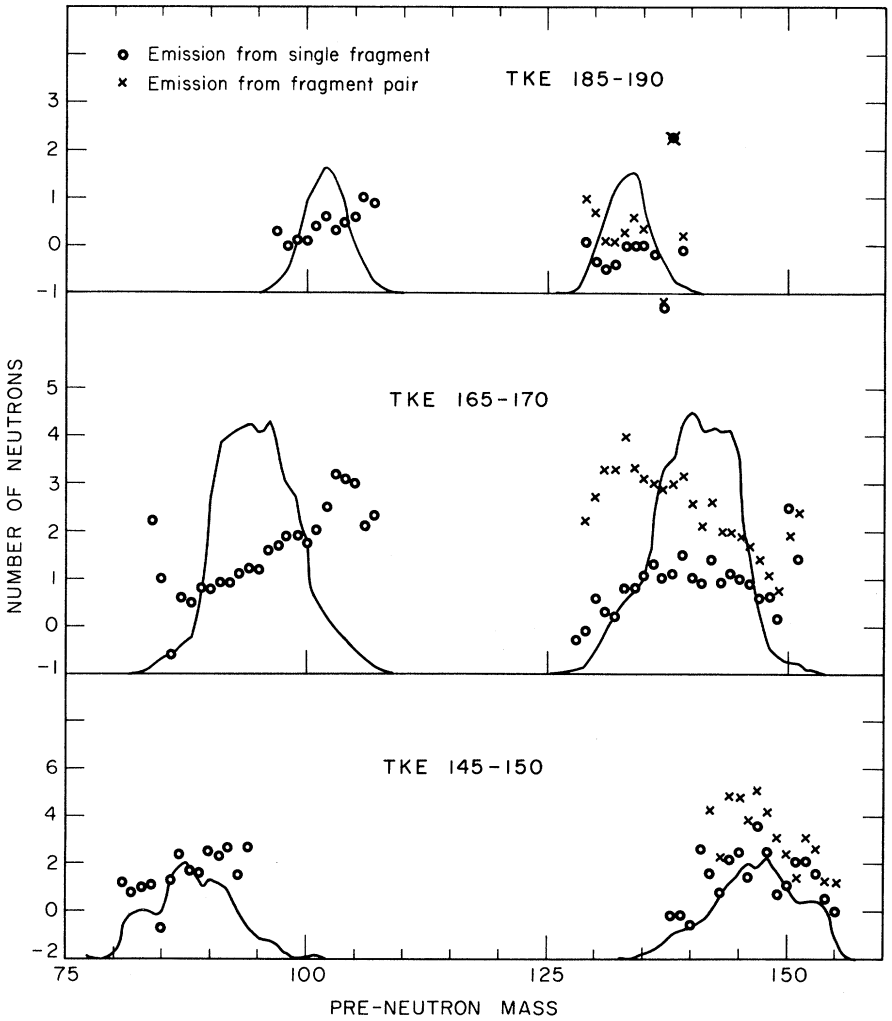

FIG. 10. Average neutron emission as a function of primary fragment mass at fixed values of primary total kinetic energy (TKE). The primary mass distributions of Fig. 9 are reproduced as solid lines.

actual width of the distributions. The relative magnitude of the dispersion effects on the wider distributions should, clearly, be much smaller.

While the resolution of the pre-neutron mass determination does not vary much with fragment mass, the post-neutron mass dispersion width increases monotonically with mass. The calculated dispersion ranges from 0.6 to 1.0 amu across the light peak, and from 1.2 to 2.2 amu across the heavy peak. These are approximate values, depending on an energy resolution figure (1.5 MeV FWHM) which is an average for solid-state detectors of this type. Again, a comparison of the dispersion widths with the observed widths of the mass distributions shows that the effect of dispersion in most cases should be very small. It is only in the 185–190-MeV distribution that the resolution at the high-mass end of the heavy peak ($\sigma \sim 1.6$ amu) is comparable with the observed width of the distribution. In this case, the high-mass tail can possibly be attributed to mass dispersion.

The variation of neutron emission with fragment mass at these same kinetic energy values is plotted in Fig. 10. In the top graph, the apparent negative neutron emission at some points in the heavy peak suggests a systematic shift of the primary mass in this mass range.

At fixed values of total kinetic energy, one would expect that the total neutron emission from complementary fragments would follow the trend of the maximum energy release as a function of fragment mass, with a maximum near mass 132. In the lower two graphs of Fig. 10 this is generally the case. However, at the higher kinetic energies, and also

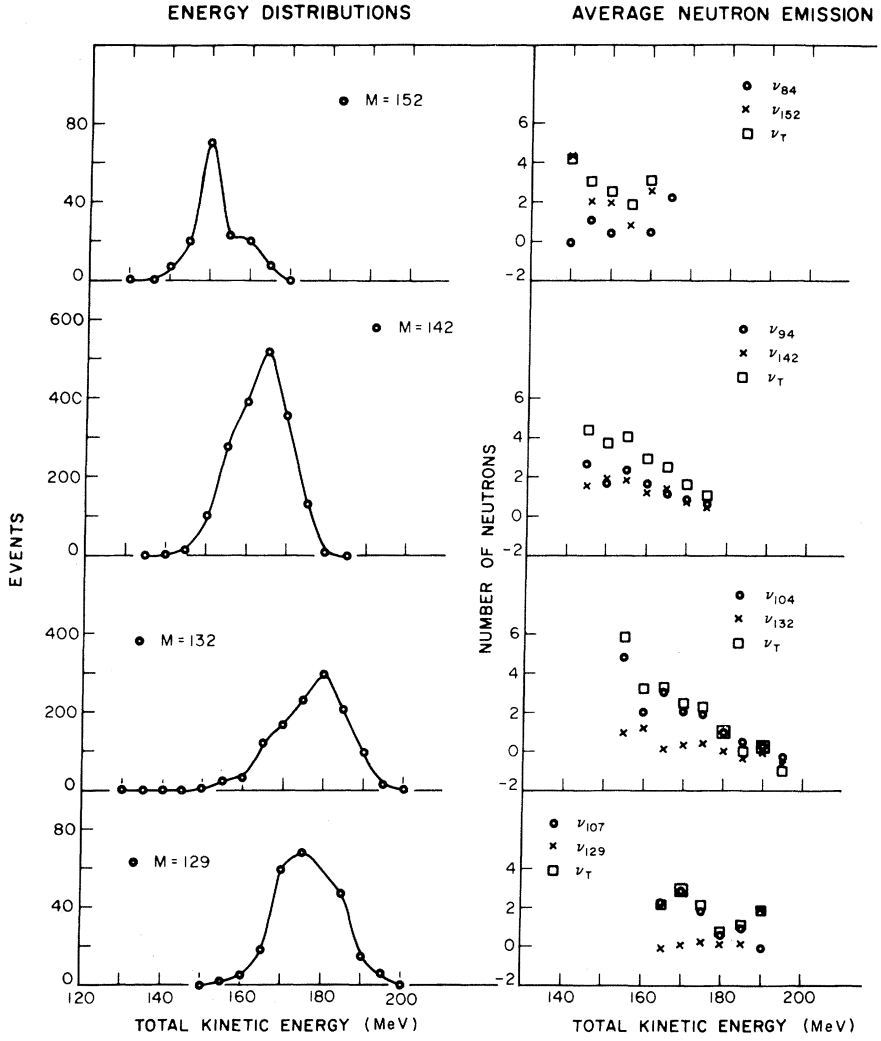

FIG. 11. Results at fixed values of primary fragment mass. Left: total-kinetic energy distributions before neutron emission. Right: average neutron emission as a function of primary total kinetic energy for complementary fragment mass pairs.

at the extreme low end of the total-kinetic energy range, the dependence upon mass of the total neutron emission deviates qualitatively from the trend of the maximum energy release. This would seem to indicate that at least for these events the charge division is determined by something other than the requirement of maximum energy release.

In Figs. 9 and 10 we have been considering variations with mass at fixed values of total kinetic energy. One can examine the same results from the opposite point of view, as is done in Fig. 11. Here we have plotted energy distributions and neutron emission as a function of total kinetic energy, at fixed values of primary fragment mass.

Both sets of results have been plotted at the same four mass divisions. The mass-142 plots are fairly typical of the results throughout most of the mass range. Mass 152 was chosen because it represents one of the highest mass ratios at which there are enough events to enable us to be relatively confident of the average neutron-emission results. Similarly, mass 129 represents the low-mass-ratio data. We plot the distributions for mass 132 in order to examine possible effects of the 50-proton, 82-neutron shell.

The energy distributions at most masses are quite symmetric, nearly Gaussian in shape. This is not true at the two wings of the mass distribution, however, where there is marked deviation from a symmetric shape. The general trends of the distributions are about what one would expect simply from the amount of energy available at different values of the ratio of heavy-to-light mass. At high mass ratios, that is, at more asymmetric divisions, where there is less energy available, the energy distribution is centered at a lower energy and is considerably narrower than those at lower mass ratios.

The plots of average neutron emission at fixed division, some of which are shown in Fig. 11, are similar to that in Fig. 6 throughout most of the mass range. However, in the vicinity of mass 132, the neutron emission comes almost exclusively from the light fragment at all kinetic energies. The low neutron emission from the heavy fragments near mass 132 has been associated with the presence of the 82-neutron shell in this mass region. The rise of total neutron emission with de-

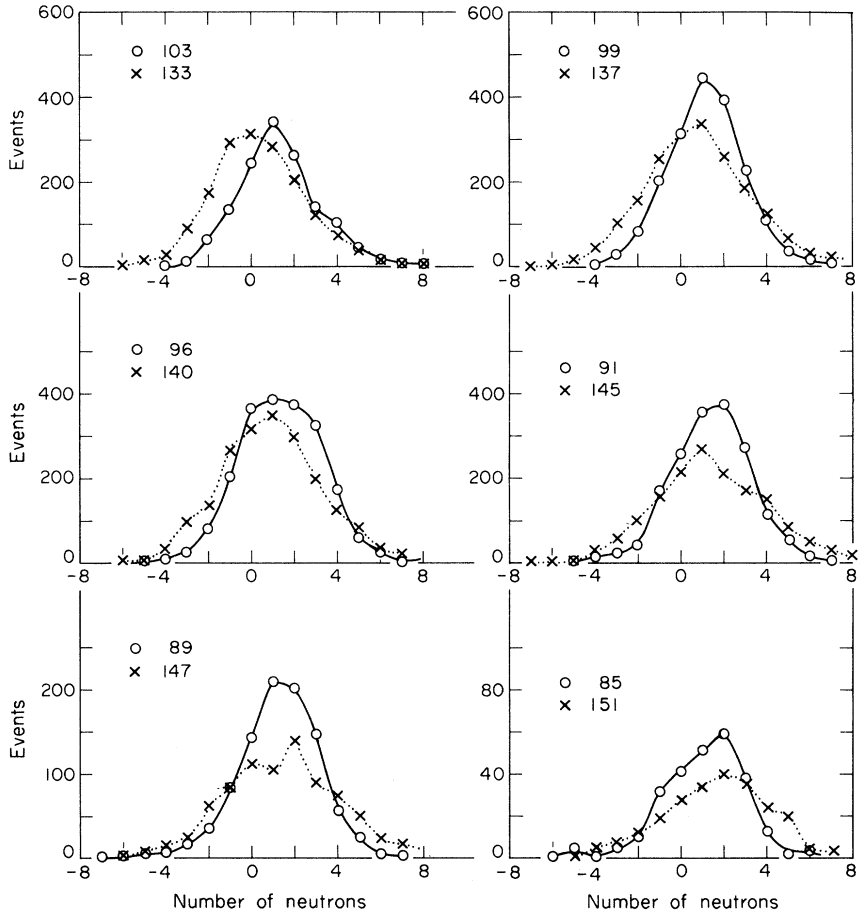

FIG. 12. Neutron number distributions from single fragments of complementary mass. Circles; light fragment. Crosses; heavy fragment.

creasing total kinetic energy is much less regular in Fig. 11 than in Fig. 6, where the results were integrated over all masses. Also, at most masses there is evidence for a leveling off or a decrease in total neutron emission at the lowest kinetic energies. This probably indicates that the events of lowest kinetic energy are characterized by charge divisions which do not produce maximum energy release.

The distribution of the number of neutrons emitted by single fragments of a given mass is indirectly related, as was stated above, to the excitation-energy distribution for fragments of that mass. In Fig. 12 we have plotted the neutron number distributions of several complementary mass pairs. The results for all masses are given in the contour diagrams of Fig. 13. The events at negative neutron numbers can, for the most part, be attributed to resolution broadening in the determination of primary and post-neutron masses.

The general trends which we find in the observed neutron number distributions are as follows: In the case of the light fragments, the distributions peak at one neutron for roughly two thirds of the mass values, and at two neutrons for the remaining mass values. We do not see any systematic trend in the alternation between peaks at one or at two neutrons. There were no observed peaks at zero in the light-fragment neutron distributions. The behavior of the distributions in the heavy-fragment case is somewhat different. For most heavy fragments below mass 140, the most probable neutron number is zero. Above mass 140, the neutron distributions usually peak at one neutron. There

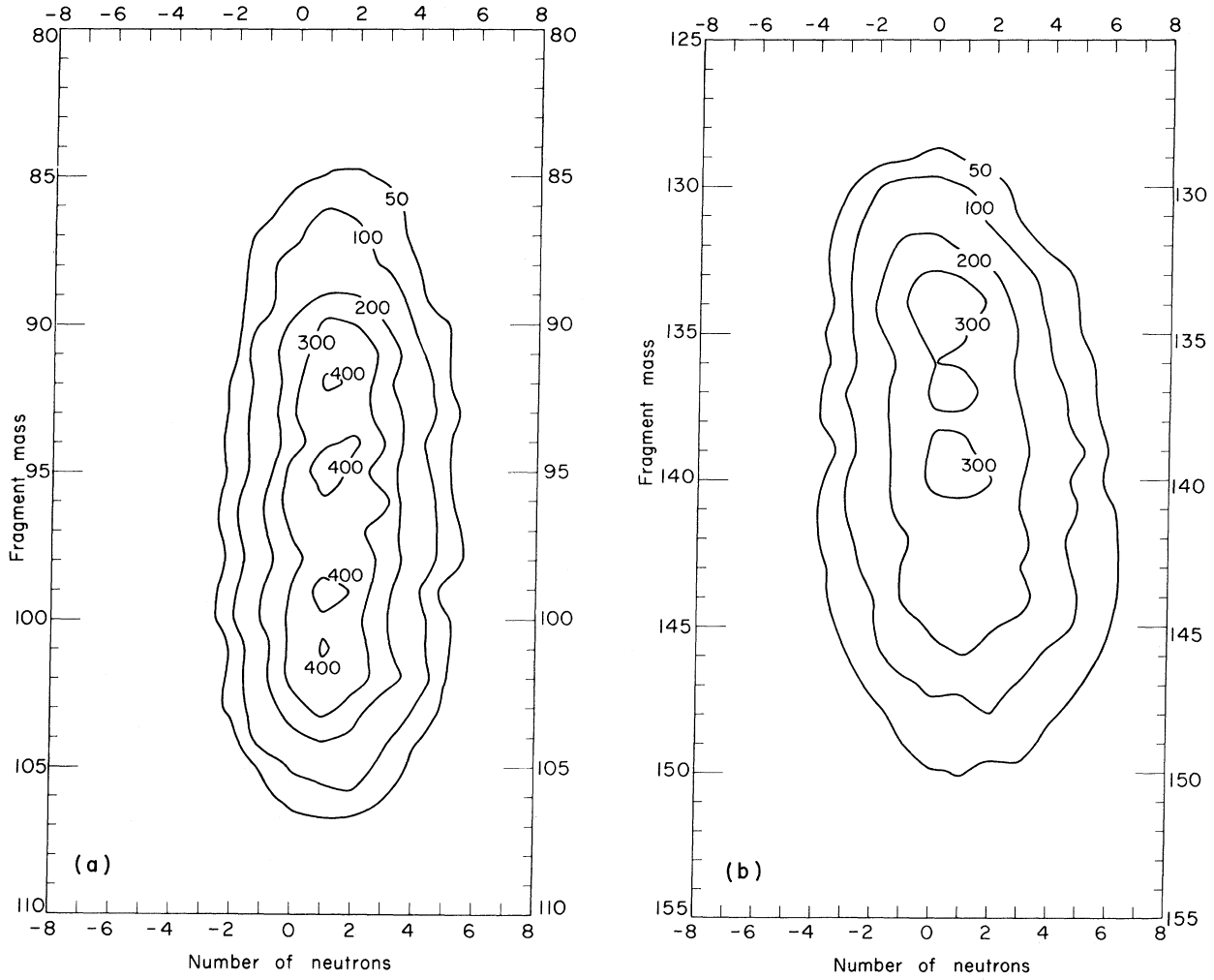

FIG. 13. Contour diagram of the number of emitted neutrons versus primary fragment mass. The number attached to the contour corresponds to events (60 000 fissions)$^{-1}$ (mass unit)$^{-1}$ (neutron)$^{-1}$. (a) Light fragment. (b) Heavy fragment.

are a few cases where a heavy-fragment distribution exhibits a peak at two neutrons, and in some of these cases there is evidence of a secondary peak at zero.

Taken at face value, the observed neutron number distributions seem to imply that the excitation energy of the light fragment is always greater than or equal to that of the complementary heavy fragment. This interpretation, however, does not take into account the possibility that the energy released in γ rays may also be mass dependent.

One further point which should be mentioned is the fact that each of the above neutron number distributions represents results within a wide range of total kinetic energy. We have also obtained neutron number distributions for events of fixed mass within 5-MeV ranges of total kinetic energy. Figure 14 is an example of the type of results obtained for masses 96 and 140. These are to be compared with the distributions for these masses given in Fig. 12. The smooth, relatively symmetric distributions of Fig. 12 are then seen to be superpositions of several distributions whose peak positions, widths, and structure vary with total kinetic energy. In general, the peaks shift to higher neutron numbers as the kinetic energy decreases.

The effect of mass dispersion on the neutron number distributions of Figs. 12 and 14 is rather larger than in the mass distributions, as can be seen by considering the distributions for the masses 96 and 140 amu, for which the calculated dispersions are 1.25 and 1.5 neutrons, respectively. The dispersion should be slightly larger at the higher fragment energies and slightly smaller at the lower energies. In the comparison with the observed distribution widths, we will use the corresponding FWHM, namely, 2.9 and 3.5 neutrons. In Fig. 12, the observed widths of the distributions are about 5 neutrons at mass 96 and 4.5 neutrons at mass 140. Upon subtraction of the contribution due to dispersion, one is left with a width of 4 at mass 96 and about 3 neutrons at mass 140. Similar procedures carried out on the distributions of Fig. 14 indicate that at the highest kinetic energies, most of the observed widths could be attributed to dispersion effects, while at the lower kinetic energies a large fraction of the observed width is real.

One question of some concern in the analysis of the neutron-emission results was the magnitude of the possible systematic error due to uncertainty in the energy calibration of the solid-state detectors. This uncertainty has been estimated[18] to be of the order of 0.5 MeV. Accordingly, the analysis was performed with modified values of the constants in the energy formula, in an attempt to assess the effect on our results. We found that these modifications did produce changes in details, but the main features summarized above were not af-

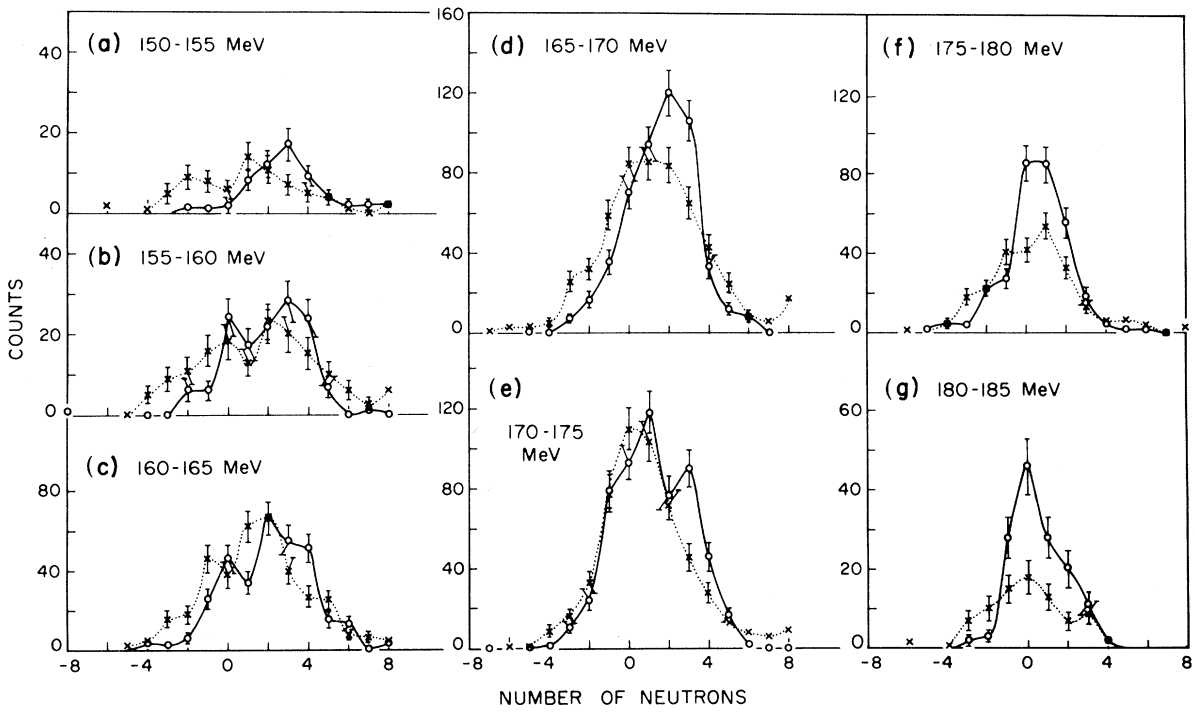

FIG. 14. Neutron number distributions from fragments of mass 96 (circles) and 140 (crosses), at different values of fragment total kinetic energy. Error bars indicate statistical error.

fected. In particular, the neutron multiplicity varied from 2.25, as in the results presented here, to 2.73, while the currently accepted value is 2.43. The effect on the neutron number distributions was to shift the peaks upward to higher neutron numbers in the analysis that gave $\bar{\nu}$ equal to 2.73. However, the observation that the peak of the neutron distribution for the heavy fragment is in general at an equal or lower number of neutrons than the peak for the complementary light-fragment distribution, seems to be preserved in the modified analysis.

One additional point to consider is the possible effect of scission neutrons on our results. As was stated previously, in any determination of primary masses, one assumes that all prompt neutrons are emitted by the fully accelerated fragments. There is some evidence, however, from measurements[19,20] of angular distributions of prompt neutrons with respect to the direction of the coincident fission fragments, that between 10 and 15% of the neutrons are not emitted by fully accelerated fragments. It has been suggested that these neutrons are emitted either before or during scission. If such is the case, it seems likely that our mass results would be affected, though the magnitude and even to some extent the nature of the effects cannot be determined without more information than is presently available. However, it is possible that the emission of scission neutrons is responsible for our low value for the average number of neutrons emitted per fission.

SUMMARY

In this experiment, primary and post-neutron fragment masses have been determined in fission of U^{235} induced by thermal neutrons. The fragment mass and energy information enabled us to obtain details of the neutron emission as a function of fragment mass and kinetic energy. This is the first time this method has been applied to the fission of U^{235}. One unique feature of this experiment is the fact that the event-by-event analysis made it possible for us to obtain distributions of the number of neutrons emitted by single fragments at each value of primary fragment mass. These distributions should be related to the single-fragment excitation-energy distributions, and have not been presented before for any fissioning nucleus.

In addition, the average neutron emission has been obtained as a function of fragment mass and total kinetic energy. We have not made a detailed comparison of our neutron emission results as a function of these two parameters with the corresponding MRC results, because the intervals of mass and energy which we used for analysis are smaller than those of MRC. We can say that our results are qualitatively similar, though there are differences in some details. In particular, we see a larger variation in total neutron emission with total kinetic energy; namely, one neutron per 11-MeV decrease in total kinetic energy, as compared with the one neutron per 18 MeV reported by MRC.

With the exception of neutron emission, the results of this experiment are contained in the arrays giving the number of events at each value of mass and total kinetic energy. These have been analyzed both as mass distributions at fixed total kinetic energy and as kinetic energy distributions at fixed mass. For the most part, the mass-distribution results confirm earlier observations; among them, the existence of structure at certain primary masses, and the conclusion that no additional mass structure is produced by neutron emission. However, the total-kinetic-energy distributions show a previously unreported deviation from symmetry at the lowest and highest mass ratios, as compared with the Gaussianlike shape throughout most of the mass range.

ACKNOWLEDGMENTS

The authors are grateful for the cooperation of the staff of the Brookhaven medical research reactor, whose cheerful assistance made this work easier in many ways. One of the authors (M.D.) thanks Brookhaven National Laboratory for enabling her to perform this work under a guest appointment. We are also indebted to Dr. Jayashree Toraskar and Ralph Stein for their assistance during the experimental run, and to John Ostrowski and Kam Ng for providing the uranium sources.

---

†Work supported by the U. S. Atomic Energy Commission.

[1]H. W. Schmitt, J. H. Neiler, and F. J. Walter, Phys. Rev. 141, 1146 (1966).

[2]H. W. Schmitt, F. Pleasonton, and R. W. Lide, Nucl. Instr. Methods 63, 237 (1968).

[3]E. Konecny and H. W. Schmitt, Phys. Rev. 172, 1213 (1968).

[4]S. C. Burnett, R. L. Ferguson, F. Plasil, and H. W. Schmitt, Phys. Rev. Letters 21, 1350 (1968).

[5]G. Andritsopoulos, T. Cornell, and A. L. Rodgers, in *Proceedings of the Symposium on the Physics and Chemistry of Fission, Salzburg, Austria, 1965* (International Atomic Energy Agency, Vienna, Austria, 1965), Vol. 1, p. 481.

[6]G. Andritsopoulos, Nucl. Phys. A94, 537 (1967).

[7]J. C. D. Milton and J. S. Fraser, in *Proceedings of the Symposium on the Physics and Chemistry of Fission, Salzburg, Austria, 1965* (International Atomic Energy Agency, Vienna, Austria, 1965), Vol. 2, p. 39.
[8]E. E. Maslin, A. L. Rodgers, and W. G. F. Core, Phys. Rev. 164, 1520 (1967).
[9]M. Derengowski and E. Melkonian, Pegram Nuclear Physics Laboratory Report No. NYO-GEN-72-191 (unpublished), p. 22.
[10]E. G. & G., Inc., Nanonotes 1, No. 2 (1964).
[11]H. W. Schmitt, W. M. Gibson, J. H. Neiler, F. J. Walter, and T. D. Thomas, in *Proceedings of the Symposium on the Physics and Chemistry of Fission, Salzburg, Austria, 1965* (International Atomic Energy Agency, Vienna, Austria, 1965), Vol. 1, p. 531.
[12]E. K. Hyde, *The Nuclear Properties of the Heavy Elements* (Prentice-Hall, Inc., Englewood Cliffs, New Jersey, 1964), Vol. 3, p. 102.
[13]J. C. D. Milton and J. S. Fraser, Phys. Rev. 111, 877 (1958).
[14]V. F. Apalin, Yu. N. Gritsyuk, I. E. Kutikov, V. I. Lebedev, and L. A. Mikaelian, Nucl. Phys. 71, 553 (1965).
[15]J. C. D. Milton, Lawrence Radiation Laboratory Report No. UCRL-9883 (unpublished).
[16]H. Maier-Liebnitz, H. W. Schmitt, and P. Armbruster, in *Proceedings of the Symposium on the Physics and Chemistry of Fission, Salzburg, Austria, 1965* (International Atomic Energy Agency, Vienna, Austria, 1965), Vol. 2, p. 143.
[17]J. Terrell, Phys. Rev. 127, 880 (1962).
[18]J. H. Neiler, F. J. Walter, and H. W. Schmitt, Phys. Rev. 149, 894 (1966).
[19]H. R. Bowman, S. G. Thompson, J. C. D. Milton, and W. J. Swiatecki, Phys. Rev. 126, 2120 (1962).
[20]K. Sharsvåg and K. Bergheim, Nucl. Phys. 45, 72 (1963).